

**Electronic Supplementary Information (ESI) for**

**Direct synthesis of an aliphatic amine functionalized metal-organic framework for efficient CO<sub>2</sub> removal and CH<sub>4</sub> purification**

Ning-Yu Huang, Zong-Wen Mo, Lu-Jian Li, Wei-Jian Xu, Hao-Long Zhou, Dong-Dong Zhou, Pei-Qin Liao\*, Jie-Peng Zhang\* and Xiao-Ming Chen

MOE Key Laboratory of Bioinorganic and Synthetic Chemistry, School of Chemistry, Sun Yat-Sen University, Guangzhou 510275, China.

\*E-mail: liaopq3@mail.sysu.edu.cn; zhangjp7@mail.sysu.edu.cn

## Supplementary Index

**Additional experimental details.**

**Scheme S1** Representation of the column breakthrough experiment.

**Figure S1.** Coordination environments of **α-Zn** and **β-Zn**.

**Figure S2.** Comparison of the PXRD patterns of **α-Cu**, **α-Zn** and **β-Zn**.

**Figure S3.** PXRD patterns of **α-Cu**.

**Figure S4.** PXRD patterns of **α-Zn**.

**Figure S5.** PXRD patterns of **β-Zn**.

**Figure S6.** TG curves of **α-Zn**, **β-Zn** and **α-Cu**.

**Figure S7.** N<sub>2</sub> adsorption and desorption isotherms of **α-Zn** and **β-Zn** at 77 K.

**Figure S8.** The CO<sub>2</sub> binding mode of **β-Zn** revealed by computational simulations.

**Figure S9.** CO<sub>2</sub> adsorption and desorption isotherms of **α-Zn** and **β-Zn**.

**Figure S10.** CH<sub>4</sub> adsorption and desorption isotherms of **α-Zn** and **β-Zn**.

**Figure S11.** Virial fitting of CO<sub>2</sub> adsorption data for (a) **α-Zn** and (b) **β-Zn**.

**Figure S12.** Virial fitting of CH<sub>4</sub> adsorption data for (a) **α-Zn** and (b) **β-Zn**.

**Figure S13.** IAST CO<sub>2</sub>/CH<sub>4</sub> selectivity of **α-Zn** and **β-Zn**.

**Figure S14.** Breakthrough curves expressed using time (min) as abscissa.

**Figure S15.** Breakthrough curves expressed using specific time (min g<sup>-1</sup>) as abscissa.

**Figure S16.** Time-dependent gas retention in the breakthrough columns.

**Figure S17.** Repeated breakthrough curves in breakthrough experiments of **β-Zn**.

**Figure S18.** Breakthrough curves of **α-Zn** for 1:99 and 1:999 CO<sub>2</sub>/CH<sub>4</sub> (v/v) mixtures.

**Table S1.** Crystallographic data and structural refinement details.

**Table S2.** The parameters of the breakthrough columns.

**Table S3.** Comparison of the CH<sub>4</sub> purification productivities of **α-Zn** and **β-Zn**.

**Table S4.** Comparison of the IAST CO<sub>2</sub>/CH<sub>4</sub> selectivity of MOFs.

**Table S5.** Comparison of the experimental CO<sub>2</sub>/CH<sub>4</sub> adsorption selectivity of MOFs.

**Table S6.** Comparison of the experimental CO<sub>2</sub>/CH<sub>4</sub> adsorption selectivity.

## Additional experimental details

**Calculation of Adsorption Enthalpy ( $Q_{st}$ ).** The Clausius-Clapeyron equation was employed to calculate the experimental adsorption enthalpy at each adsorption amount  $n$ :

$$\left[ \frac{\partial \ln p}{\partial (1/T)} \right]_n = -\frac{Q_{st}}{R} \quad (\text{S-1})$$

Where  $p$  is the pressure,  $T$  is the temperature and  $R$  is the universal gas constant.

Method 1: direct calculation from isotherm data points:

$$Q_{st} = (\ln p_2 - \ln p_1) \frac{RT_1 T_2}{T_2 - T_1} \quad (\text{S-2})$$

Method 2: Virial fitting:

$$\ln p = \ln n + \frac{1}{T} \sum_{i=0}^m a_i n^i + \sum_{j=0}^l b_j n^j \quad (\text{S-3})$$

Where  $a_i$  and  $b_i$  are virial coefficients and  $m$  and  $l$  are the number of coefficients used to describe the isotherms.

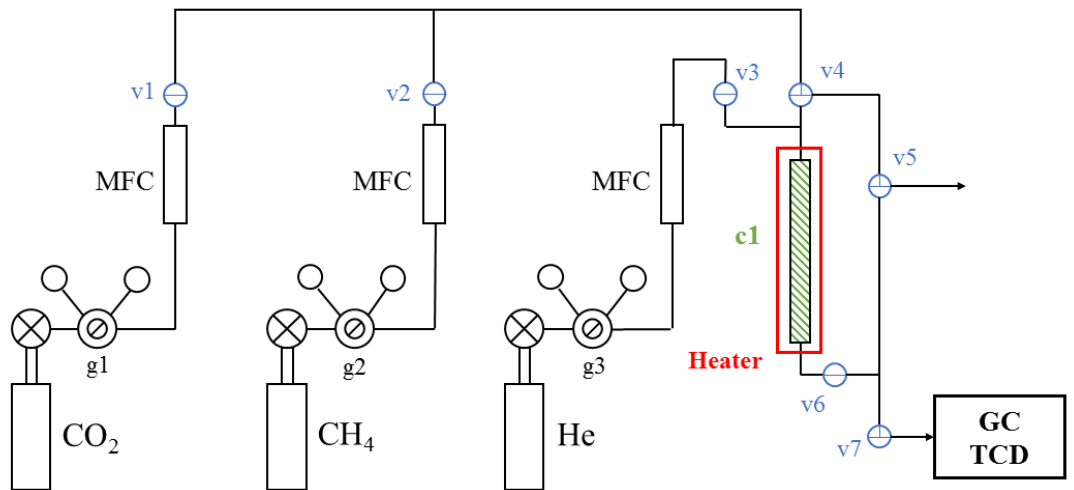
The adsorption enthalpy is obtained from the following equation derived from the Clausius-Clapeyron equation.

$$Q_{st} = -R \left[ \frac{\partial \ln p}{\partial \left( \frac{1}{T} \right)} \right]_n = -R \sum_{i=0}^m a_i n^i \quad (\text{S-4})$$

**Breakthrough Experiments.** The breakthrough experiments were carried out using the reported set up,<sup>1, 2</sup> in which the sample column was filled with powder sample with negligible pressure drop observed. The column parameters are listed in Table S2. Before the breakthrough experiment, the column was activated by passing He and heated at 373 K for 5 hours, and then cooled to the measurement temperature of 298(1) K. Ultra-high-purity CH<sub>4</sub> and CO<sub>2</sub> were mixed in the pipeline to give the mixed gas (40:60 CO<sub>2</sub>/CH<sub>4</sub> and 10:90 CO<sub>2</sub>/CH<sub>4</sub>; flow rate 1.0 cm<sup>3</sup> min<sup>-1</sup>). The gas stream at the outlet of the column was collected by a six-way valve and analyzed online by a gas chromatography (Agilent 7890A) with a TCD detector (G3440A) and a PLOT/Q column. The detection limit of TCD is 1 ppm, which is calibrated by commercially mixed gas (1 ppm CH<sub>4</sub>, N<sub>2</sub> as balanced gas). The error of TCD is lower than 1% RSD based on the equipment index.

The flow rate of gas mixture at the inlet, which was controlled by mass flow controllers, was defined as  $v_i$ . Prior to the breakthrough experiments, gas mixture was directly introduced to GC and the detected peak area was defined as  $S_i$ . During breakthrough experiments, the gas mixture at the outlet was introduced to GC and the detected peak area was defined as  $S_o$ . Therefore, the relative flow rate at the outlet was  $v_i*(S_o/S_i)$ . For example, when the flow rate at the inlet was 1.0  $\text{mL min}^{-1}$ , the flow rate at the outlet was  $(S_o/S_i)*1.0 \text{ mL min}^{-1}$ .

The calculation methods for the gas adsorption capacity and gas purification productivity were reported in our previous studies.<sup>1, 2</sup>



$v$  = stop valve;  $g$  = pressure gauge;  $c$  = sample packed column

MFC = Mass Flow Controller

**Scheme S1** Representation of the column breakthrough experiment.

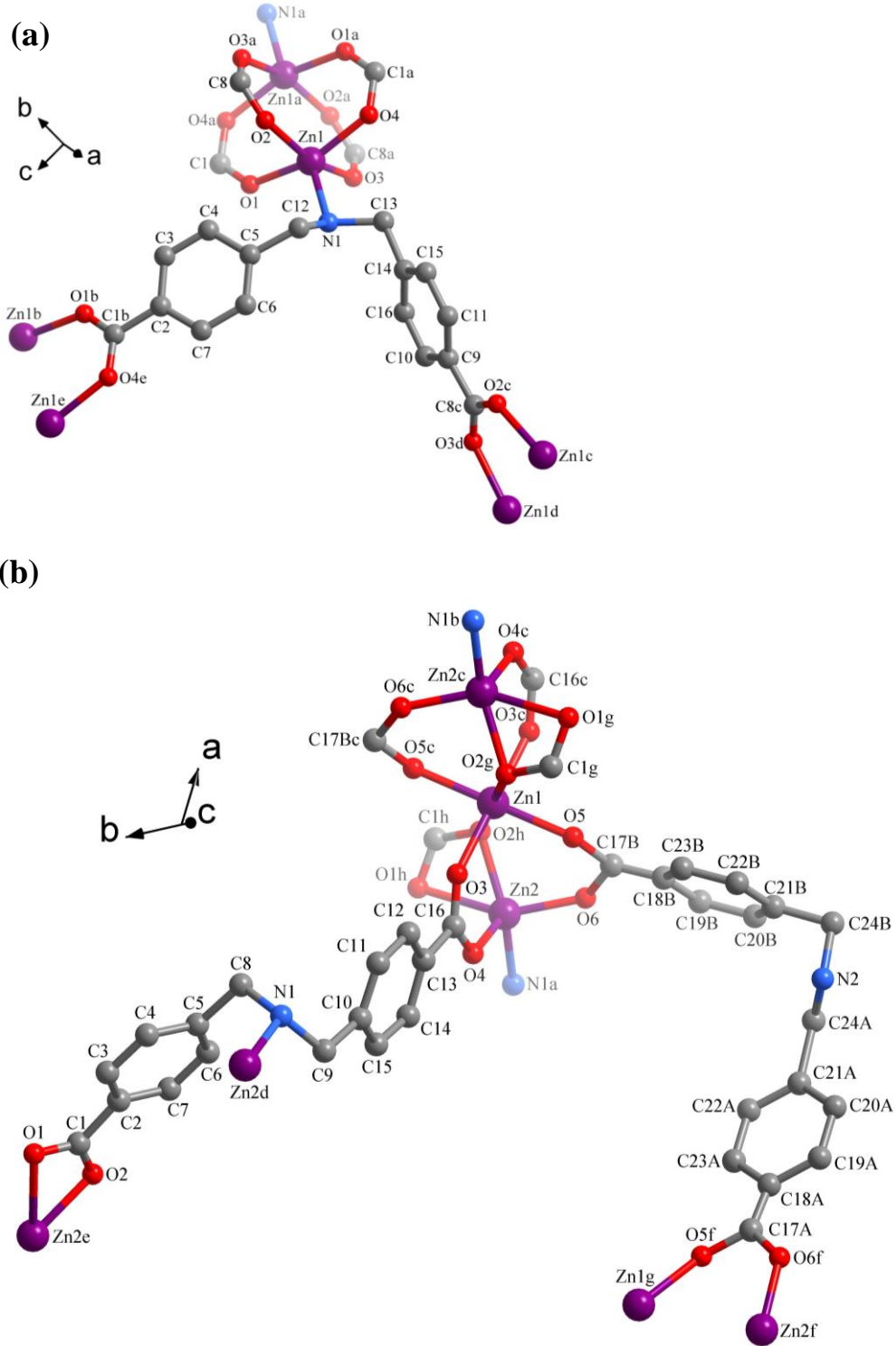


**Figure S1** (a) Perspective views of the coordination environments of  $\alpha$ -Zn. Symmetry codes: a =  $-x, 1-y, -z$ ; b =  $-x, 1-y, 1-z$ ; c =  $2/3+x-y, 1/3+x, 1/3-z$ ; d =  $-1/3-x+y, 1/3-x, 1/3+z$ ; e =  $x, y, 1+z$ ; (b) Perspective views of the coordination environments of  $\beta$ -Zn. Symmetry codes: a =  $2/3-x+y, 4/3-x, -2/3+z$ ; b =  $1+x-y, x, 1-z$ ; c =  $5/3-x, 4/3-y, 1/3-z$ ; d =  $4/3-y, 2/3+x-y, 2/3+z$ ; e =  $y, 1-x+y, -z$ ; f =  $1/3+x-y, -1/3+x, 2/3-z$ ; g =  $2/3-x+y, 4/3-x, 1/3+z$ ; h =  $1+x-y, x, -z$ .

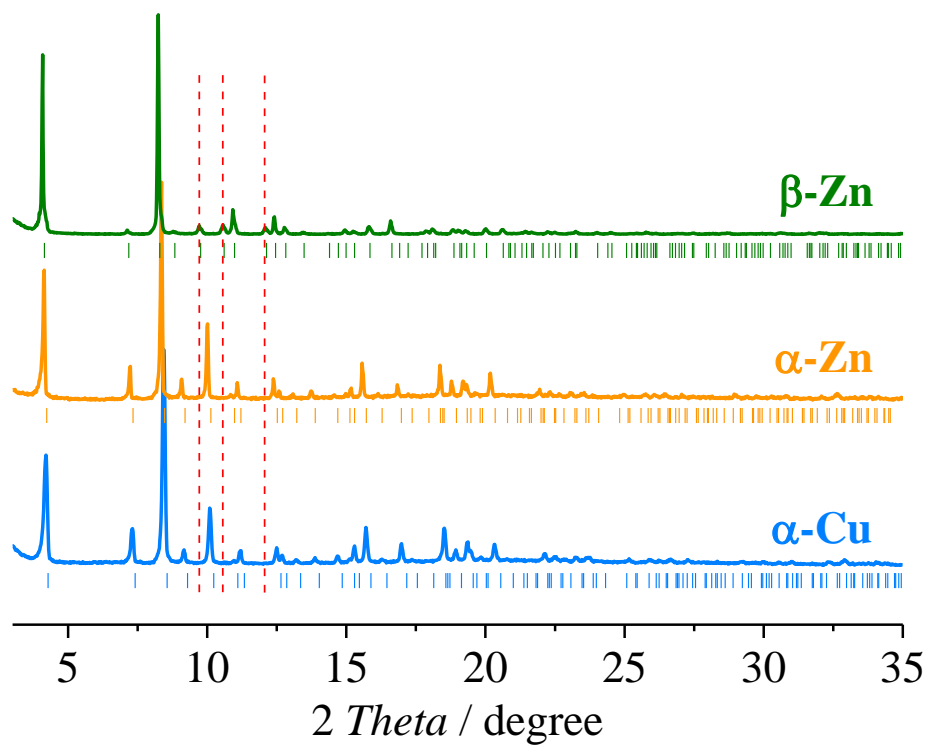


**Figure S2** Comparison of PXRD patterns of  $\alpha$ -Cu,  $\alpha$ -Zn and  $\beta$ -Zn.

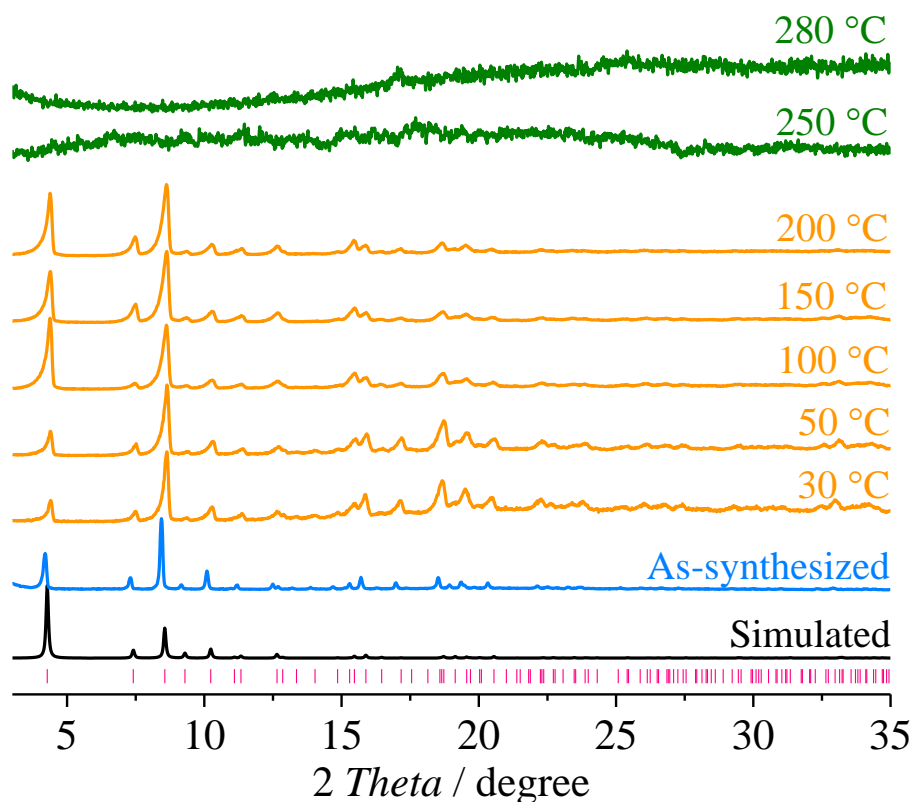


**Figure S3** PXRD patterns of  $\alpha$ -Cu.

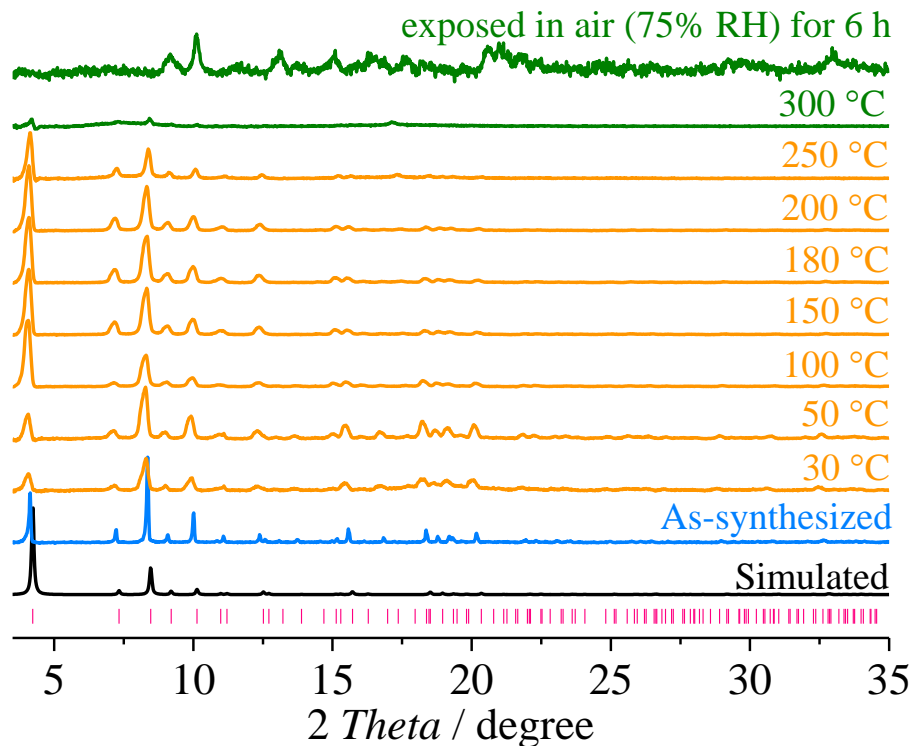


**Figure S4** PXRD patterns of  $\alpha$ -Zn.

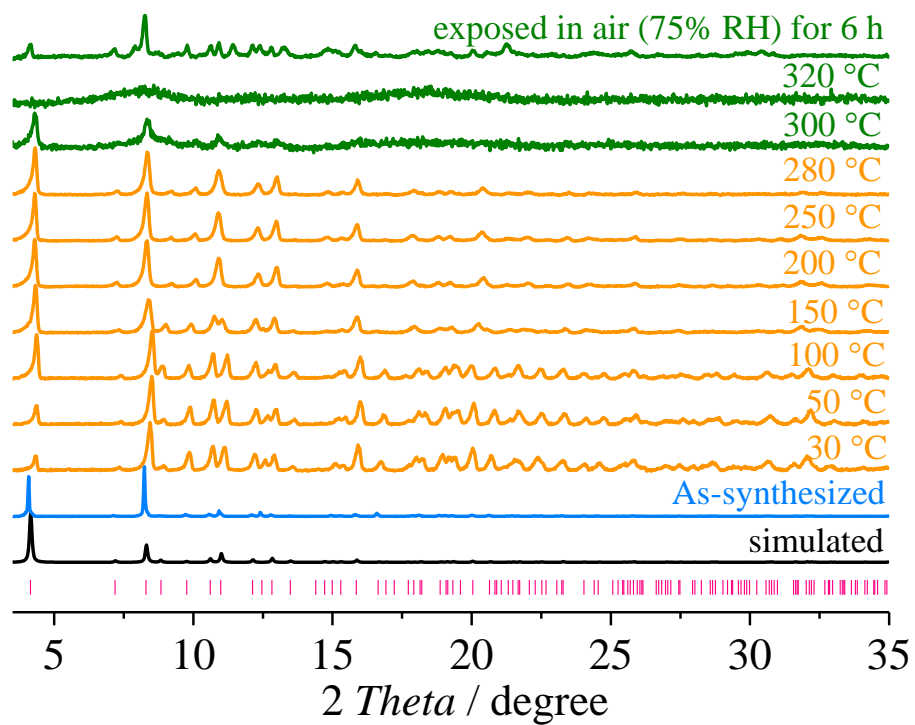


**Figure S5** PXRD patterns of  $\beta$ -Zn.

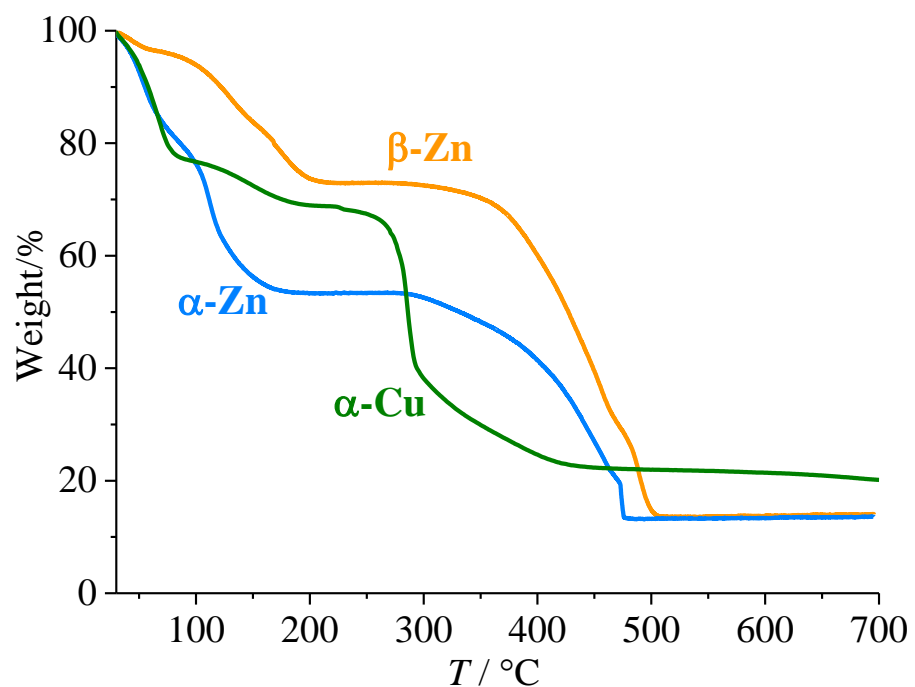


**Figure S6** TG curves of  $\alpha$ -Zn,  $\beta$ -Zn and  $\alpha$ -Cu.

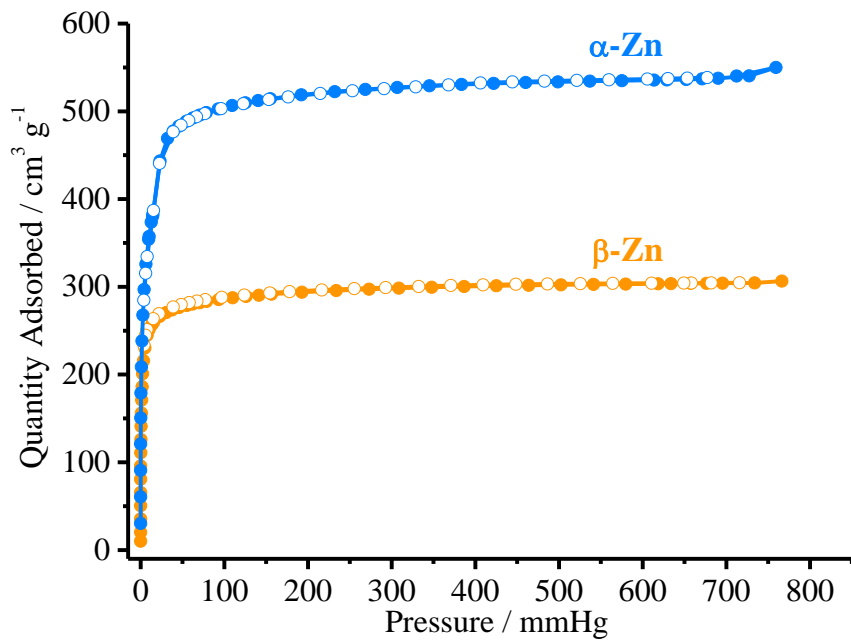


**Figure S7** Nitrogen adsorption (solid) and desorption (open) isotherms of  $\alpha$ -Zn and  $\beta$ -Zn at 77 K.

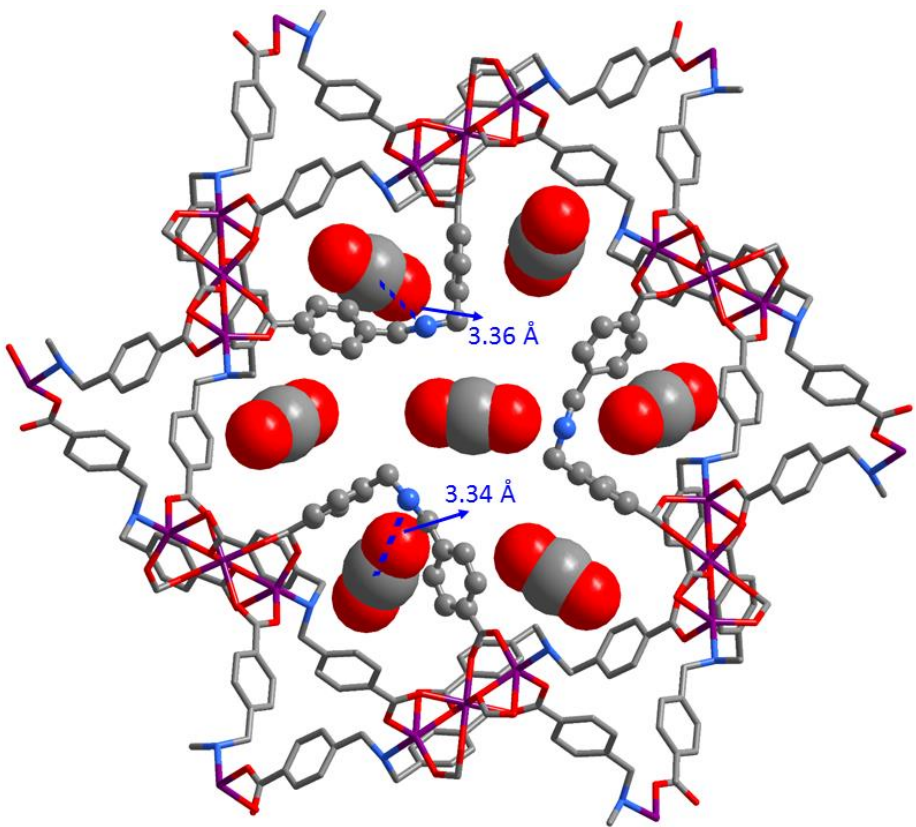


**Figure S8.** The  $\text{CO}_2$  binding mode of  $\beta\text{-Zn}$  revealed by computational simulations.

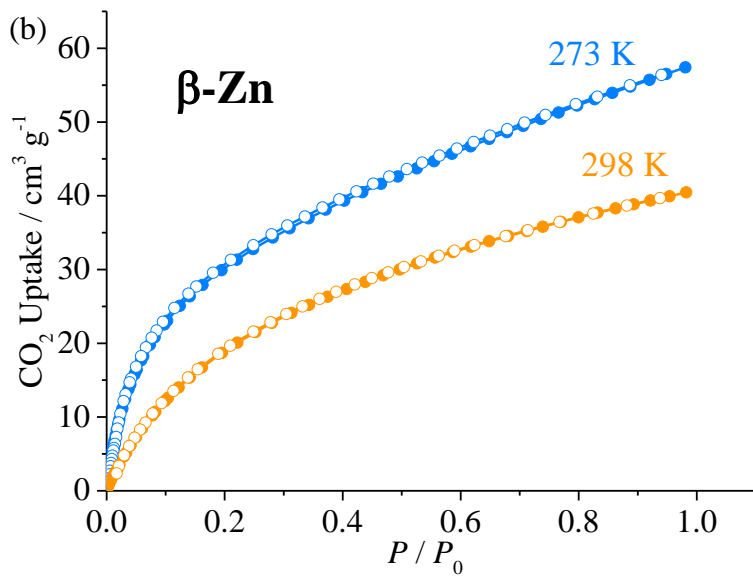
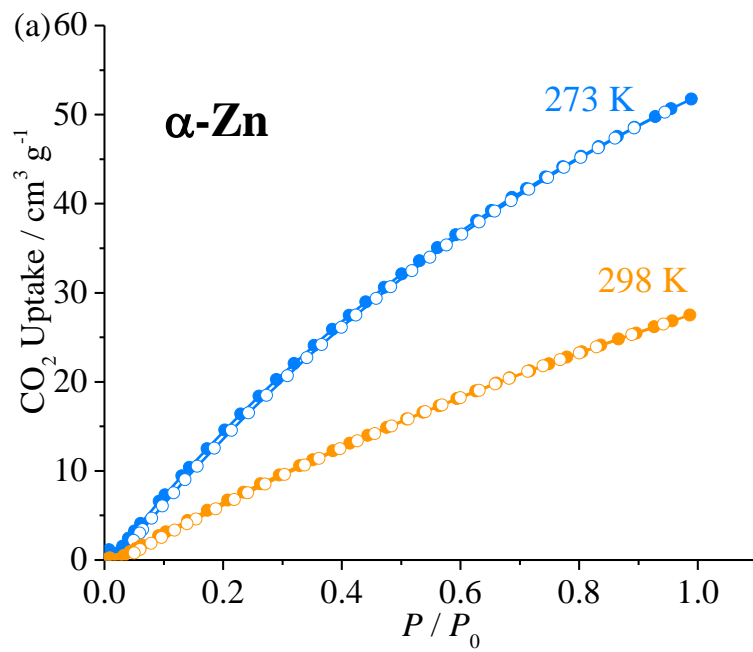


**Figure S9** CO<sub>2</sub> adsorption (solid) and desorption (open) isotherms of (a)  $\alpha\text{-Zn}$  and (b)  $\beta\text{-Zn}$ .

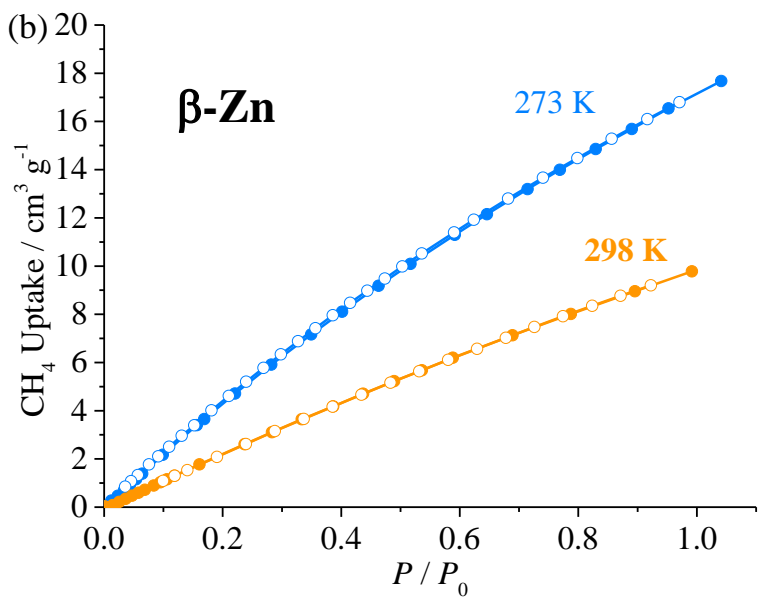
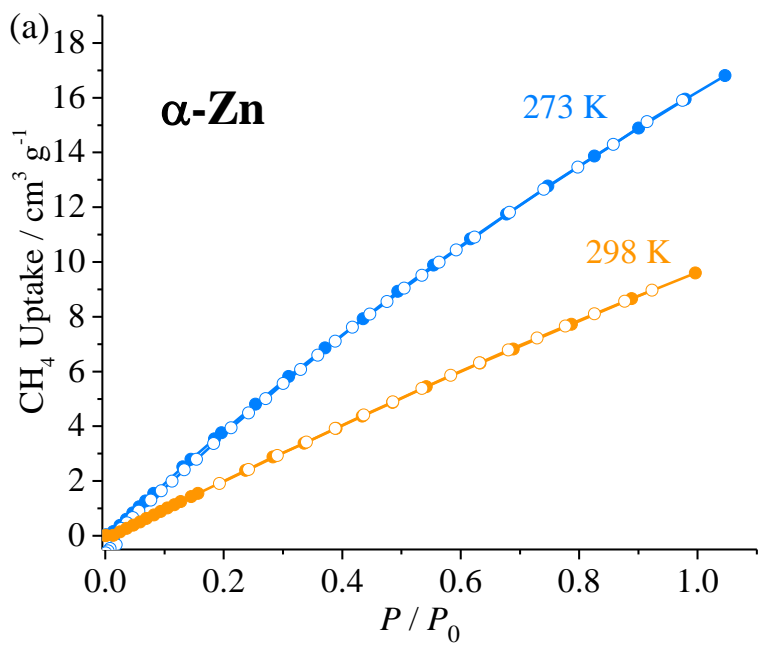


**Figure S10**  $\text{CH}_4$  adsorption (solid) and desorption (open) isotherms of (a)  $\alpha\text{-Zn}$  and (b)  $\beta\text{-Zn}$ .

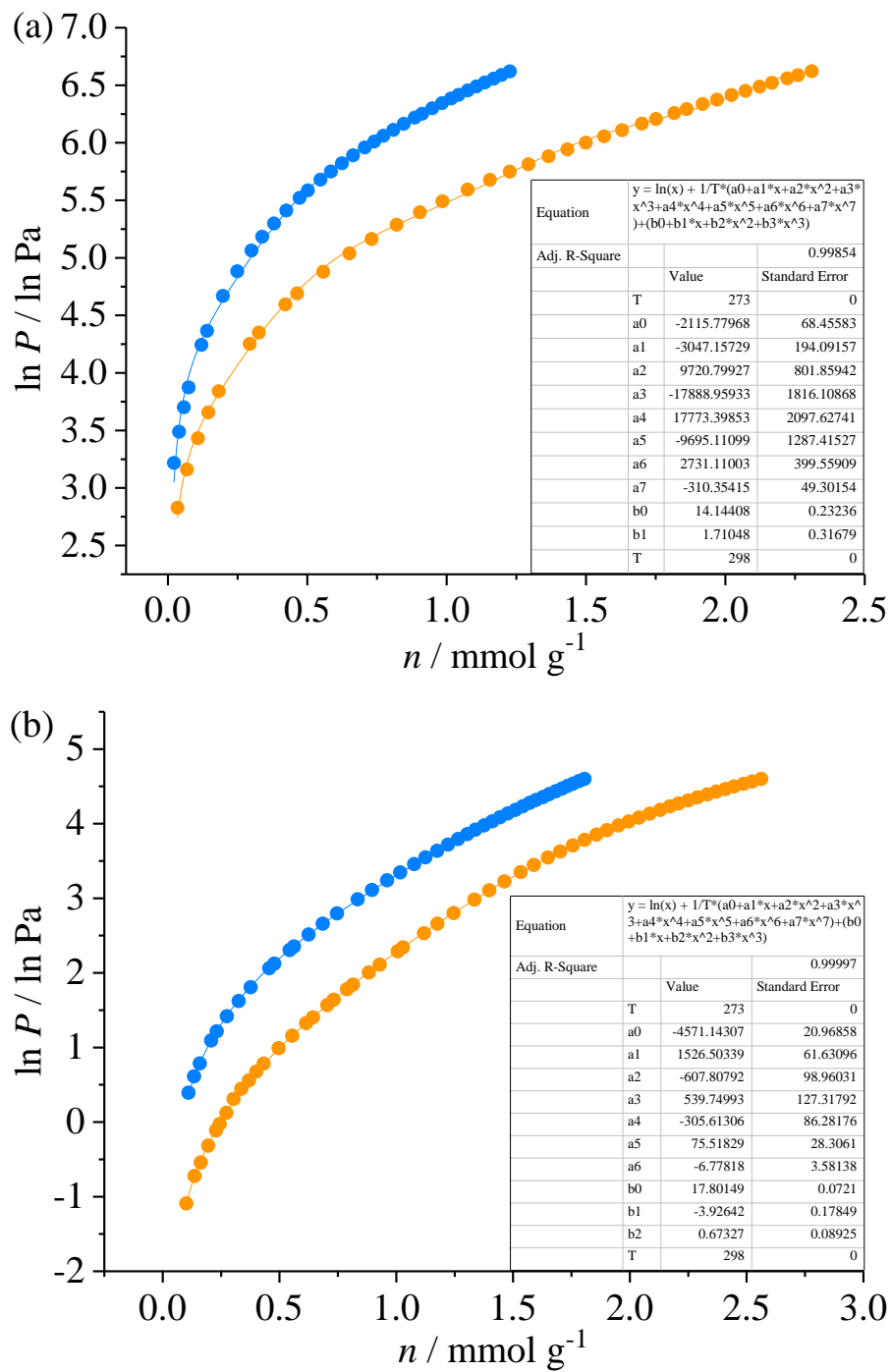


**Figure S11.** Virial fitting of CO<sub>2</sub> sorption data for (a)  $\alpha$ -Zn and (b)  $\beta$ -Zn.

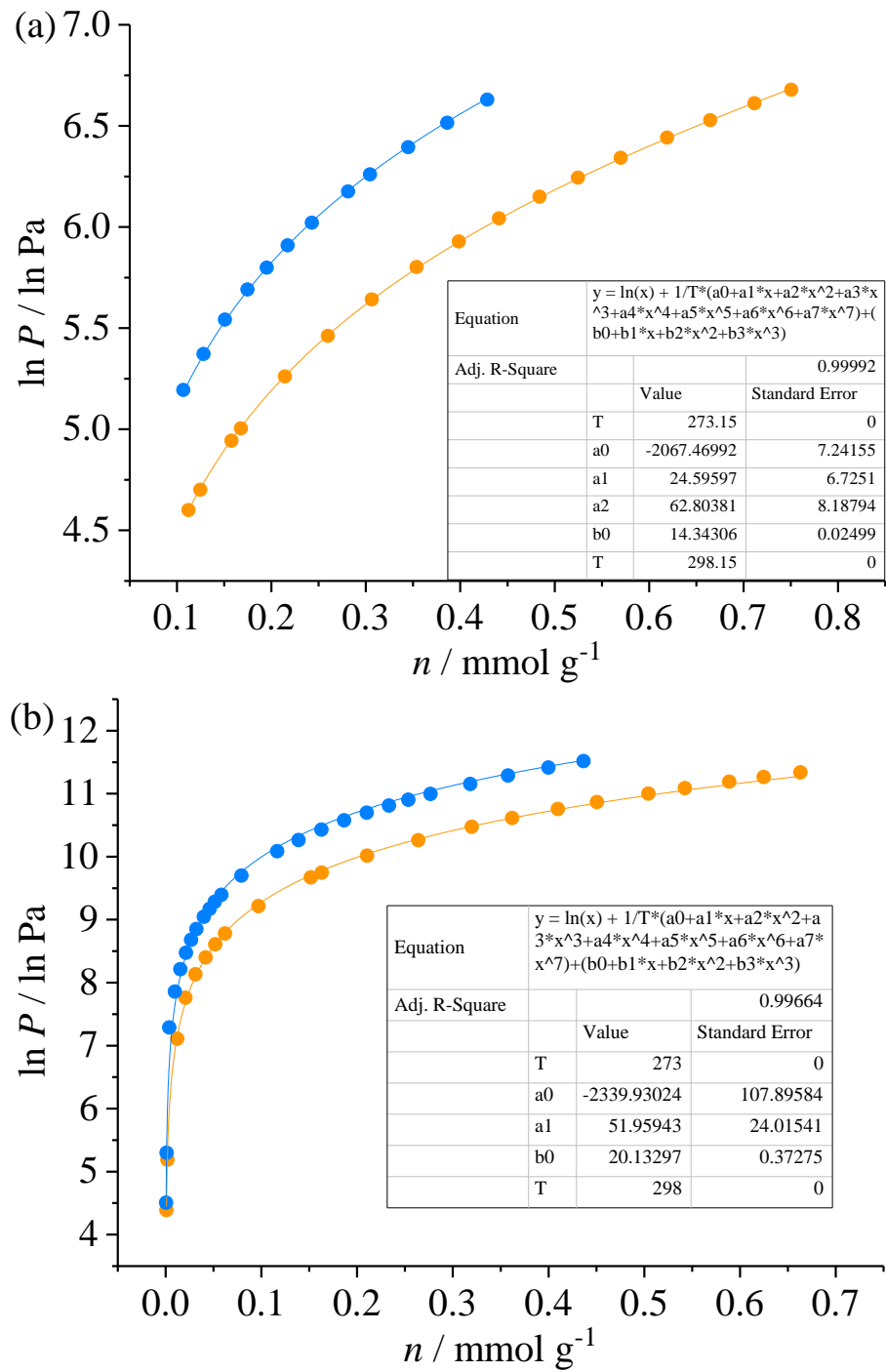


**Figure S12.** Virial fitting of CH<sub>4</sub> sorption data for (a)  $\alpha$ -Zn and (b)  $\beta$ -Zn.

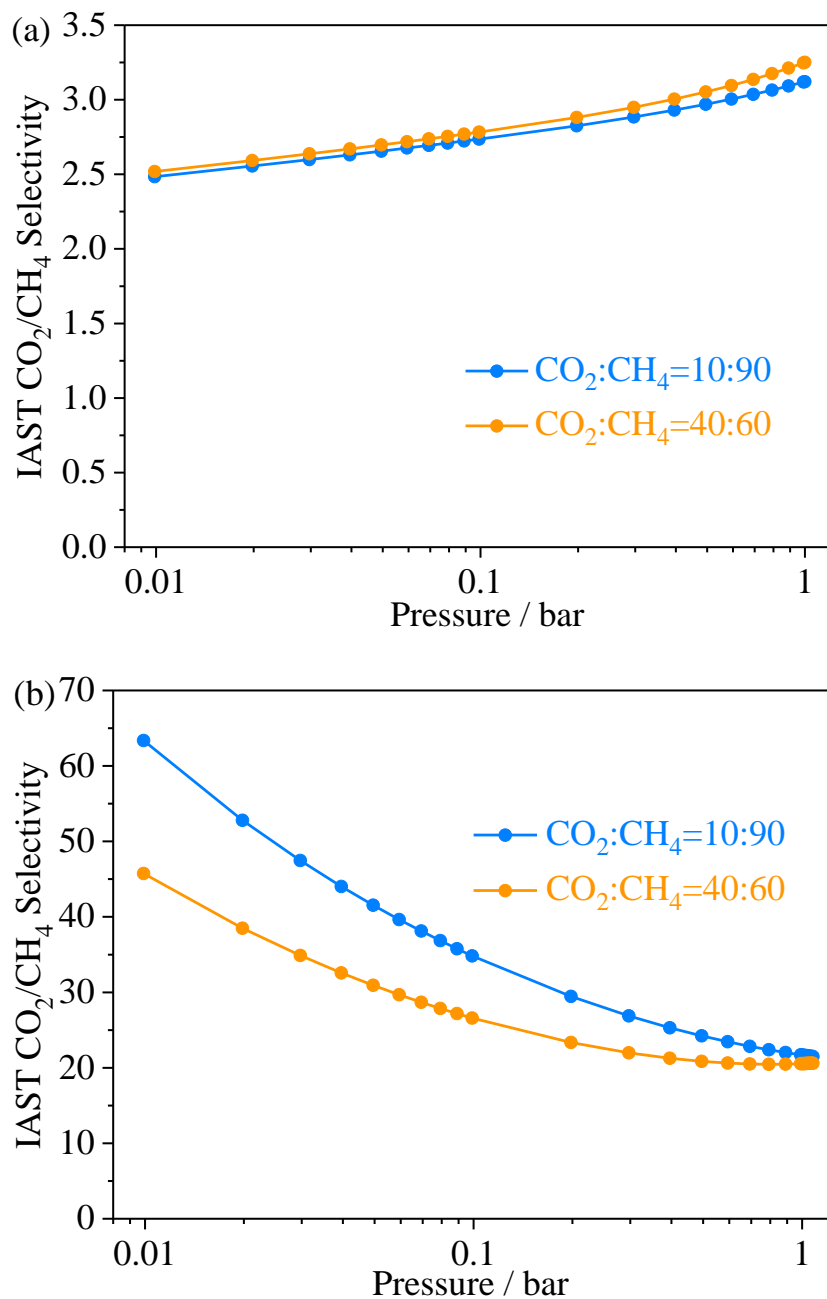


**Figure S13** IAST CO<sub>2</sub>/CH<sub>4</sub> selectivity of (a)  $\alpha$ -Zn and (b)  $\beta$ -Zn.

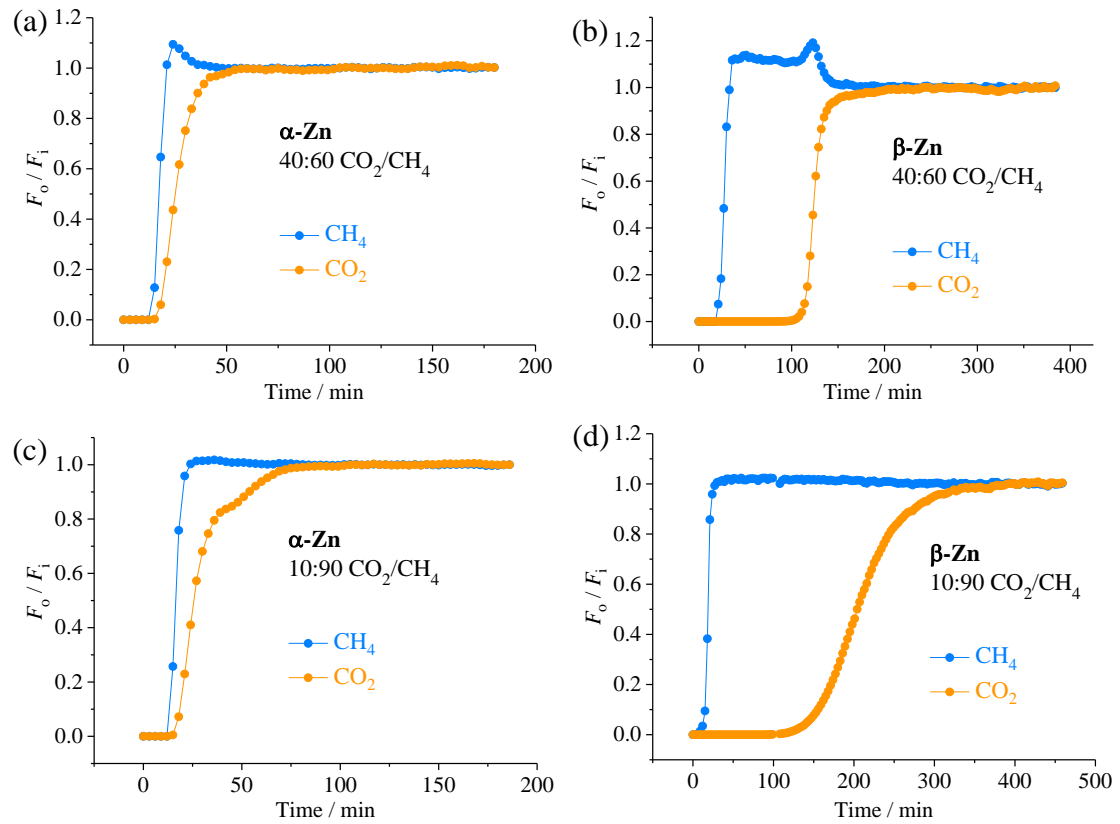


**Figure S14** Breakthrough curves of (a) Fig. 3a, (b) Fig. 3b, (c) Fig. 4a and (d) Fig. 4b expressed using time (min) as abscissa.

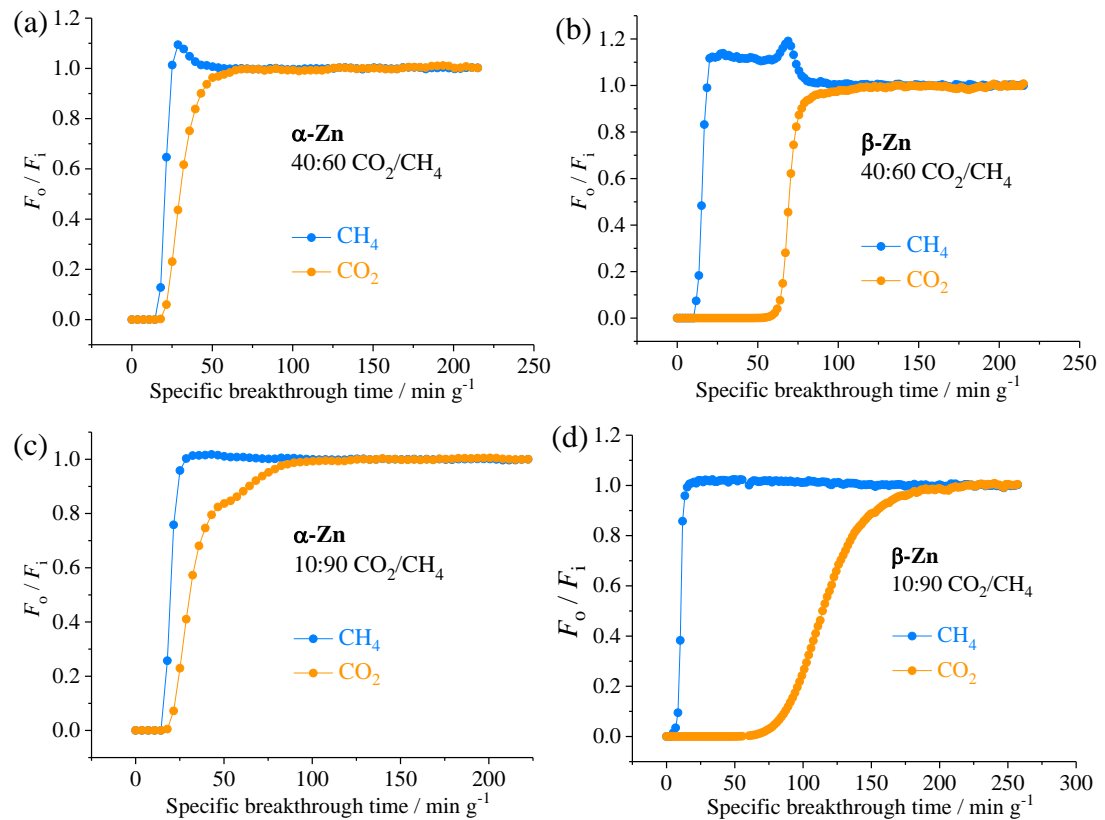


**Figure S15** Breakthrough curves of (a) Fig. 3a, (b) Fig. 3b, (c) Fig. 4a and (d) Fig. 4b expressed using specific breakthrough time ( $\text{min g}^{-1}$ ) as abscissa.

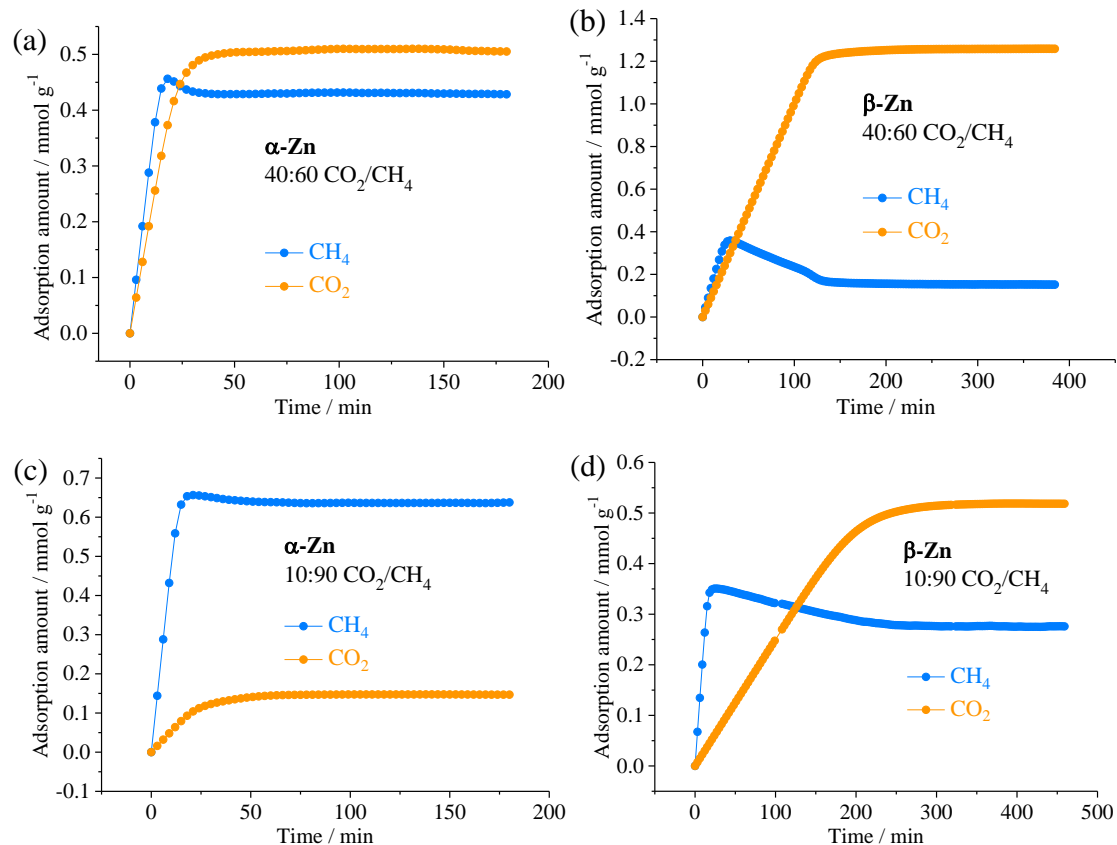


**Figure S16** Time-dependent gas retention of the breakthrough columns, obtained by integration of the breakthrough curves of experiments of (a) Fig. 3a, (b) Fig. 3b, (c) Fig. 4a and (d) Fig. 4b.

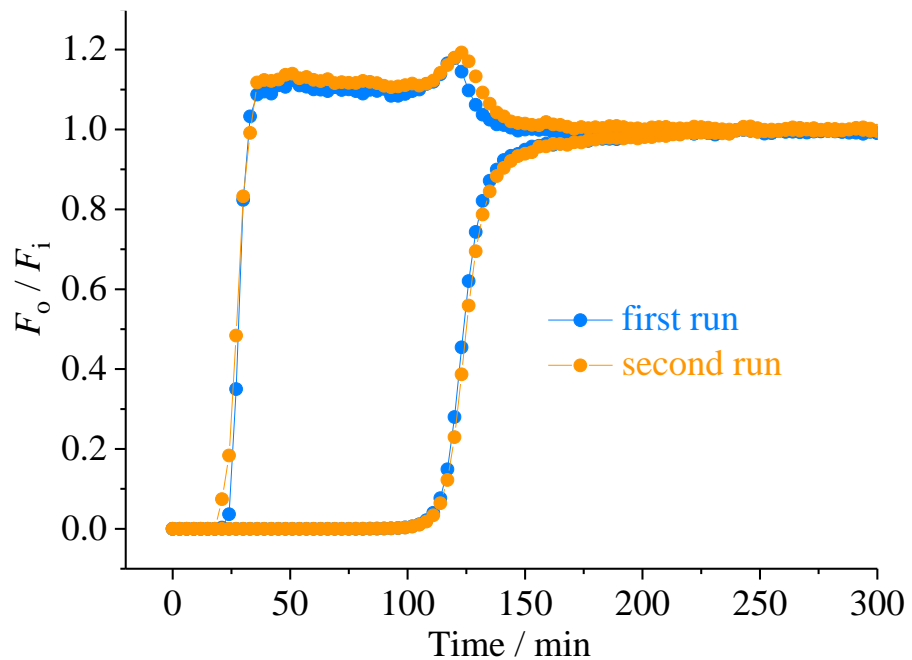


**Figure S17.** Repeated breakthrough curves in breakthrough experiments of  $\beta\text{-Zn}$  for 40:60  $\text{CO}_2/\text{CH}_4$  ( $v/v$ ) mixtures at 298 K and 1 bar. Lines are drawn to guide the eye.  $F_i$  and  $F_o$  are the flow rates of each gas at the inlet and outlet, respectively. The column was regenerated by passing He at 298 K for 12 hours.

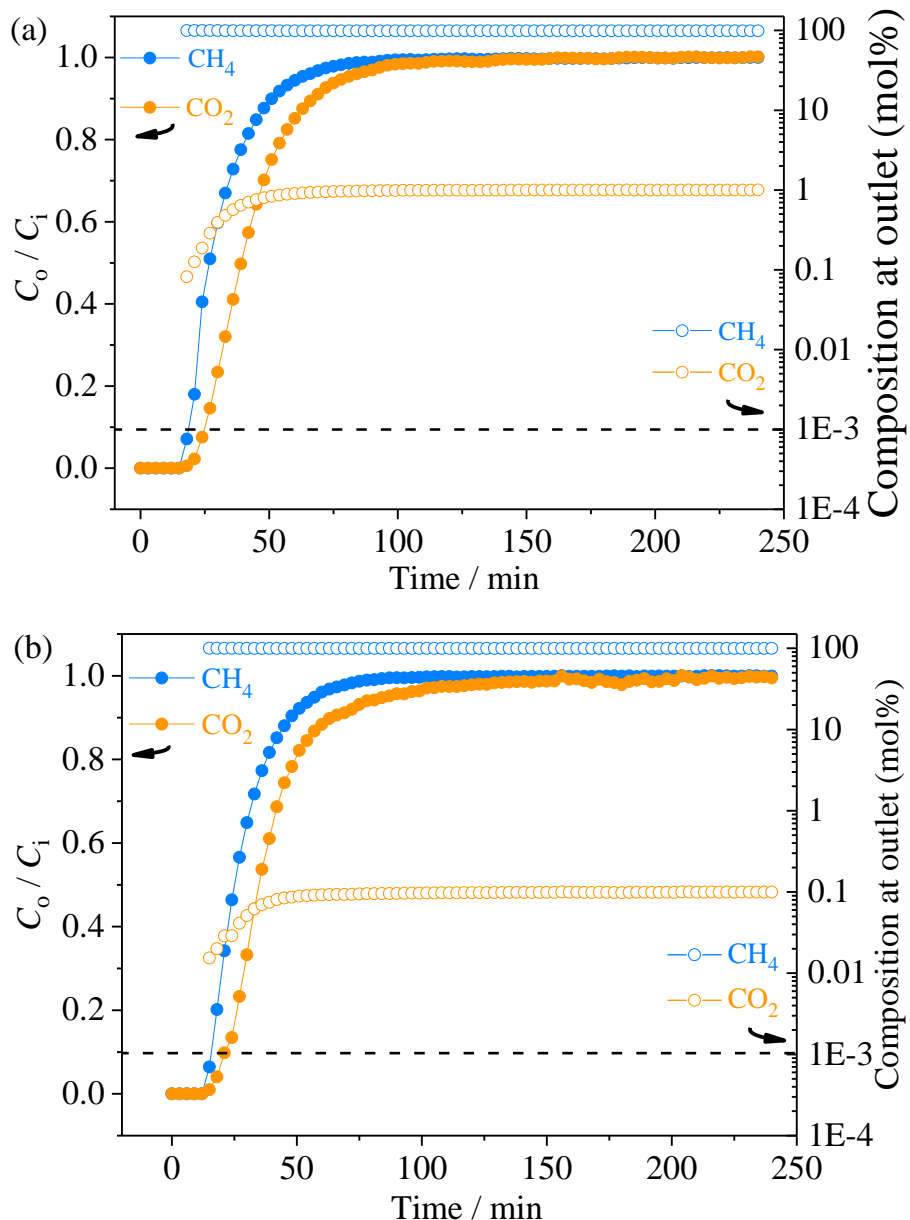


**Figure S18.** Breakthrough curves (solid) and composition at outlet (open) in breakthrough experiments of  $\alpha$ -Zn for (a) 1:99 and (b) 1:999  $\text{CO}_2/\text{CH}_4$  ( $v/v$ ) mixtures at 298 K and 1 bar. Lines are drawn to guide the eye.  $C_i$  and  $C_o$  are the concentrations of each gas at the inlet and outlet, respectively. Dashed lines highlight the composition at 0.001%, corresponding to the composition of other gases at 99.999%.

**Table S1** Crystallographic data and structural refinement details

Compound	<b><math>\alpha</math>-Zn</b>	<b><math>\beta</math>-Zn</b>	<b><math>\alpha</math>-Cu<sup>1</sup></b>
Formula	C <sub>16</sub> H <sub>13</sub> NO <sub>4</sub> Zn	C <sub>48</sub> H <sub>39</sub> N <sub>3</sub> O <sub>12</sub> Zn <sub>3</sub>	C <sub>16</sub> H <sub>13</sub> CuNO <sub>4</sub>
Formula weight	348.64	1045.93	364.84
Space group	<i>R</i> -3	<i>R</i> -3	<i>R</i> -3
Temperature (K)	203	203	223
<i>a</i> /Å	41.740(4)	42.4897(8)	41.28(2)
<i>c</i> /Å	9.958(1)	10.4000(4)	9.864(4)
<i>V</i> /Å <sup>3</sup>	15025(4)	16260.4(9)	14556.7
<i>Z</i>	18	9	18
$\rho_{\text{calc}}$ (g cm <sup>-3</sup> )	0.694	0.961	/
reflns coll.	27125	29635	/
unique reflns	5169	5024	/
$\mu$ (mm <sup>-1</sup> )	1.093	1.515	/
$R_{\text{int}}$	0.0354	0.0384	/
$R_1$ [ $I > 2\sigma(I)$ ] <sup>[a]</sup>	0.0411	0.0608	/
$wR_2$ [ $I > 2\sigma(I)$ ] <sup>[b]</sup>	0.1282	0.2030	/
$R_1$ (all data)	0.0419	0.0708	/
$wR_2$ (all data)	0.1292	0.2140	/
GOF	1.098	1.093	/

<sup>a</sup> $R_1 = \sum ||F_o| - |F_c|| / \sum |F_o|$ . <sup>b</sup> $wR_2 = [\sum w(F_o^2 - F_c^2)^2 / \sum w(F_o^2)^2]^{1/2}$

**Table. S2** The parameters of the breakthrough columns studied in this work.

Materials & mixed-gas	Gas	Gas retention (mmol g <sup>-1</sup> )	Column volume (mmol)	Sample weight (g)	Sample density (g cm <sup>-3</sup> )	Sample volume (cm <sup>3</sup> )	Gas in dead space (mmol g <sup>-1</sup> )	Sample uptake (mmol g <sup>-1</sup> )
<b>α-Zn</b> 10:90	CH <sub>4</sub>	0.638	0.306	0.837	0.694	1.206	0.276	0.362
	CO <sub>2</sub>	0.147					0.031	0.116
<b>α-Zn</b> 40:60	CH <sub>4</sub>	0.428					0.184	0.244
	CO <sub>2</sub>	0.505					0.123	0.382
<b>β-Zn</b> 10:90	CH <sub>4</sub>	0.276	0.340	1.785	0.961	1.857	0.133	0.143
	CO <sub>2</sub>	0.518					0.015	0.503
<b>β-Zn</b> 40:60	CH <sub>4</sub>	0.152					0.089	0.063
	CO <sub>2</sub>	1.258					0.059	1.199

Gas retention was calculated based on the integration of the breakthrough curves.<sup>1, 2</sup>

Column volume was calculated based on the gas retention of Ar by using the same setup except that the sample column was empty;

Sample volume = Sample weight/Sample density;

Gas in dead space = (Column volume – Sample volume/22.4)/Sample weight;

Sample uptake = Gas retention – Gas in dead space.

**Table. S3** Comparison of the CH<sub>4</sub> purification productivities of **α-Zn** and **β-Zn**.

			Gravimetric/Volumetric productivity (mmol g <sup>-1</sup> /mmol cm <sup>-3</sup> )		
Materials	Crystal density (g cm <sup>-3</sup> )	CO <sub>2</sub> /CH <sub>4</sub>	99.999%+	99.9%+	99%+
<b>α-Zn</b>	0.694	10:90	—	—	0.088/0.061
		40:60	—	—	—
<b>β-Zn</b>	0.961	10:90	1.49/1.43	2.32/2.23	3.14/3.02
		40:60	0.75/0.72	0.95/0.91	1.40/1.34

**Table. S4** Comparison of the IAST CO<sub>2</sub>/CH<sub>4</sub> selectivity of different MOFs at 1 bar. The IAST selectivity better than that of **β-Zn** were highlighted in blue.

Materials	CO <sub>2</sub> uptake at 1 bar (cm <sup>3</sup> g <sup>-1</sup> )	CH <sub>4</sub> uptake at 1 bar (cm <sup>3</sup> g <sup>-1</sup> )	CO <sub>2</sub> :CH <sub>4</sub> (v:v)	Temperature (K)	IAST selectivity	Ref.
<b>α-Zn</b>	27.48	9.60	10:90	298	3.12	<b>this work</b>
			40:60		3.25	
<b>β-Zn</b>	40.46	9.78	10:90	298	21.68	
			40:60		20.55	
SIFSIX-3-Zn	57	16	50:50	298	<b>231</b>	<i>Nature</i> , <b>2012</b> , 495, 80
SIFSIX -2-Cu-i	120	9.7	50:50	298	<b>33</b>	
SIFSIX -2-Cu	41	6.9	50:50	298	5.3	
ZIF-69	41	12	50:50	298	5.6	<i>Coord. Chem. Rev.</i> <b>2011</b> , 255, 1791
ZIF-78	51	14.5	50:50	298	10.5	
ZIF-82	54	11.5	50:50	298	9.8	
JUC-199	40	11	50:50	298	9	<i>J. Mater. Chem. A</i> , <b>2016</b> , 4, 15240
MOF-5	44.8	—	50:50	RT	2.3	<i>Energy Environ. Sci.</i> , <b>2011</b> , 4, 2177
HKUST-1	56.0	—	50:50	RT	6.5	
MAF-4	17.9	—	50:50	RT	4.7	

**Table. S5** Comparison of the experimental CO<sub>2</sub>/CH<sub>4</sub> adsorption selectivity of different MOFs. The experimental selectivity better than that of **β-Zn** were highlighted in blue.

Materials	Gas uptake (CO <sub>2</sub> /CH <sub>4</sub> , cm <sup>3</sup> g <sup>-1</sup> )		CO <sub>2</sub> :CH <sub>4</sub> (v:v)	Temperature & Pressure	Selectivity	Ref.
	Mixed-gas	Single-component				
<b>α-Zn</b>	2.5/7.8	27.48/9.60	10:90	298 K 1 bar	2.9 <sup>a</sup>	this work
	8.5/5.6		40:60		2.3 <sup>a</sup>	
<b>β-Zn</b>	11.3/3.3	40.46/9.78	10:90		32 <sup>a</sup>	
	26.8/1.5		40:60		29 <sup>a</sup>	
MAF-42	12/0.5	16/5	40:60	298 K 1 bar	28 <sup>b</sup>	<i>Nat. Commun.</i> , <b>2015</b> , 6, 6350
oxidized MAF-42 (O100)	5/~/0	5/~/0			700 <sup>b</sup>	
SIFSIX-3-Zn	56/—	57/16	50:50	298 K	350 <sup>b</sup>	<i>Nature</i> , <b>2012</b> , 495, 80
SIFSIX-2-Cu-i	70/—	120/9.7	50:50	1 bar	51 <sup>a</sup>	
CCP-1 (coordination polymers)	—/—	19/4.0	5:95	298 K 2 bar	89 <sup>a</sup>	<i>Chem. Sci.</i> , <b>2017</b> , 8, 3109
			10:90		42 <sup>a</sup>	
			20:80		15 <sup>a</sup>	
			50:50		2 <sup>a</sup>	
Cu-BTC	22/7.8	—/—	25:75	308 K 3 bar	6.37 <sup>a</sup>	<i>Sep. Purif. Technol.</i> , <b>2015</b> , 146, 136
MIL-53(Al)	29/4.5	—/—	50:50	303 K 1 bar	7.0 <sup>b</sup>	<i>Microporo. Mesopor. Mat.</i> , <b>2009</b> , 120, 221
ZJNU-54a.	120/	26/	50:50	298 K 1 bar	5.2	<i>Dalton Trans.</i> , <b>2016</b> , 45, 13373
MOF-74-Ni	—/—	—/—	50:50	303 K 1 bar	15 <sup>a</sup>	<i>J. Phys. Chem. C</i> , <b>2012</b> , 116, 26636
MOF-74-Co					12 <sup>a</sup>	
MOF-74-Zn					9 <sup>a</sup>	
STA-12-Ni					6 <sup>a</sup>	
LIFM-10(Cu)	~110/~17	65.9/20.7	50:50	298 K 1 bar	7.9 <sup>b</sup>	<i>Chem. Eur. J.</i> , <b>2016</b> , 22, 16147
LIFM-11(Cu)	~75/~10	78.0/19.1			5.7 <sup>b</sup>	
MIL-91(Ti)	—/—	67/7	50:50	303 K 1 bar	18 <sup>b</sup>	<i>J. Mater. Chem. A</i> , <b>2016</b> , 4, 1383
Al-BDC	—/—	—/—	50:50	303 K 1 bar	10.5 <sup>a</sup>	<i>Sep. Sci. Technol.</i> , <b>2015</b> , 50, 874

<sup>a</sup>: breakthrough experiments, <sup>b</sup>: mixed-gas adsorption.

**Table. S6** Comparison of the experimental CO<sub>2</sub>/CH<sub>4</sub> adsorption selectivity of porous adsorbent materials. The experimental selectivity better than that of **β-Zn** were highlighted in blue.

Materials	Gas uptake (CO <sub>2</sub> /CH <sub>4</sub> , cm <sup>3</sup> g <sup>-1</sup> )		CO <sub>2</sub> :CH <sub>4</sub> (v:v)	Temperature & Pressure	Selectivity	Ref.
	Mixed-gas	Single-component				
<b>α-Zn</b>	2.5/7.8	27.48/9.60	10:90	298 K 1 bar	2.9 <sup>a</sup>	this work
	8.5/5.6		40:60		2.3 <sup>a</sup>	
<b>β-Zn</b>	11.3/3.3	40.46/9.78	10:90		32 <sup>a</sup>	
	26.8/1.5		40:60		29 <sup>a</sup>	
Zeolite 5A	47/4.0	—/—	40:60	303 K 1.2 bar	56 <sup>b</sup>	<i>Microporo.</i> <i>Mesopor.</i> <i>Mat., 2014,</i> 200, 1
Zeolite NaX	103/1.6	96/—	50:50	303 5 bar	61 <sup>a</sup>	<i>Ind. Eng.</i> <i>Chem. Res.</i> <b>2014</b> , 53, 9860
Zeolite EMC-1	116/2.2	108/—			41 <sup>a</sup>	
Zeolite NaUSY	42/3.6	27/—			12 <sup>a</sup>	
Zeolite SAPO-37	85/6.7	63/—			14 <sup>e</sup>	
Zeolite DAY	20/4.7	11/—			5 <sup>a</sup>	
T-type Zeolite	—/—	90/17	50:50	288 K 1 bar	17.05 <sup>b</sup>	<i>Chem. Eng.</i> <i>J., 2013,</i> 230, 380
Zeolite 13X	96/9	—/—	50:50	313 K 2 bar	11.3 <sup>a</sup>	<i>Microporo.</i> <i>Mesopor.</i> <i>Mat., 2014,</i> 187, 100
Porous carbon Li@GDY-NH <sub>2</sub>	—/—	83/—	50:50	298 K 1 bar	14.7 <sup>b</sup>	<i>ACS Appl.</i> <i>Mater.</i> <i>Interfaces</i> <b>2017</b> , 9, 30002
Activated carbon beads	—/—	49/22	50:50	303 K 100 kPa	3.6 <sup>a</sup>	<i>J. Chem.</i> <i>Eng. Data,</i> <b>2015</b> , 60, 2684

<sup>a</sup>: breakthrough experiments, <sup>b</sup>: mixed-gas adsorption.

## References

1. P.-Q. Liao, H. Chen, D.-D. Zhou, S.-Y. Liu, C.-T. He, Z. Rui, H. Ji, J.-P. Zhang and X.-M. Chen, *Energy Environ. Sci.*, 2015, **8**, 1011-1016.
2. P.-Q. Liao, N.-Y. Huang, W.-X. Zhang, J.-P. Zhang and X.-M. Chen, *Science*, 2017, **356**, 1193-1196.